Electronic Supplementary Material (ESI) for Soft Matter.

Supporting Information

Against the Rules: Pressure Induced Transition from High to Reduced Order

Frederik Neuhaus,[a,b] Dennis Mueller,[a] Radu Tanasescu,[a] Cristina Stefaniu,[c] Pierre-Léonard Zaffalon,[a] Sandor Balog,[d] Takashi Ishikawa,[e] Renate Reiter,[f] Gerald Brezesinski[c] and Andreas Zumbuehl*[a,b]

a Department of Chemistry, University of Fribourg, Chemin du Musée 9, 1700 Fribourg, Switzerland
b National Center of Competence in Research in Chemical Biology, Quai Ernest Ansermet 30, 1211 Geneva, Switzerland
c Max Planck Institute of Colloids and Interfaces Research Campus Potsdam-Golm, 14476 Potsdam, Germany
d Adolphe Merkle Institute, University of Fribourg, Chemin du Verdiers 4, 1700 Fribourg, Switzerland
e Paul Scherrer Institute (PSI) OFLB/010, 5232 Villigen PSI, Switzerland
f University of Freiburg, Experimental Polymer Physics, Hermann Herder Strasse 3, 79104 Freiburg, Germany

Abstract: Predicting the properties of a bilayer membrane from the phospholipid molecular structure requires more in-depth information on the fundamental physical forces at play. Acquiring this knowledge is essential for envisioning new generations of drug delivery nano-containers. The close linkage between the synthesis of new artificial phospholipids and highly sensitive physical-chemical analytical methods allows to define molecular interactions and to establish the relationship between the chemical structure and physical-chemical properties. In this context, with the aim of increasing the number of hydrogen bond donors compared to natural phospholipids, a phospholipid compound bearing urea moieties has been synthesized. The new molecules self-assemble at soft interfaces in thin layers with distinctive structural order, and in bulk in interdigitated bilayers. An uncommon phase sequence LE (disordered state) – exothermic transition - LC_1 (highly ordered) – endothermic transition - LC_2 (reduced order) is observed during compression at low temperatures. The observed strong change in membrane thickness (thin LC_1 phase, thicker LC_2 phase) together with the presence of a strong hydrogen bond network of the headgroups in LC_1, requires a revision of the two-dimensional Clausius-Clapeyron equation. This shows that a small change in molecular structure can lead to a significant change in membrane biophysics.

DOI: 10.1039/xx0x0000xx

Table of Contents 2

Experimental Procedures

1. General Information

The starting compounds and solvents were purchased from Sigma-Aldrich/Fluka, ABCR, TCI Chemicals or Acros and were used without further purification. For reactions under inert gas conditions, the solvents (dichloromethane and chloroform) were dried over molecular sieves 4 Å and degassed afterwards. Column chromatography was carried out using 230−400 mesh, 60 Å silica gel (Brunschwig). TLC plates (Merck, Silica gel 60 F254) were developed with $KMnO_4$-solution. ^{1}H, ^{13}C and ^{31}P NMR spectra were recorded (as indicated) on either a Bruker 300 or 400 MHz spectrometer and are reported as chemical shifts in ppm relative to the signal of the deuterated NMR-solvent. Spin multiplicities are reported as singlet (*s*), doublet (*d*), triplet (*t*), with coupling constants (*J*) given in Hz, or multiplets (*m*). Broad peaks are marked as *br*. HRESI-MS was performed on a QSTAR Pulsar (AB/MDS Sciex) spectrometer and are reported as mass-per-charge ratio m/z. IR spectra were recorded on a PerkinElmer Spectrum One FT-IR spectrometer (ATR, Golden Gate).

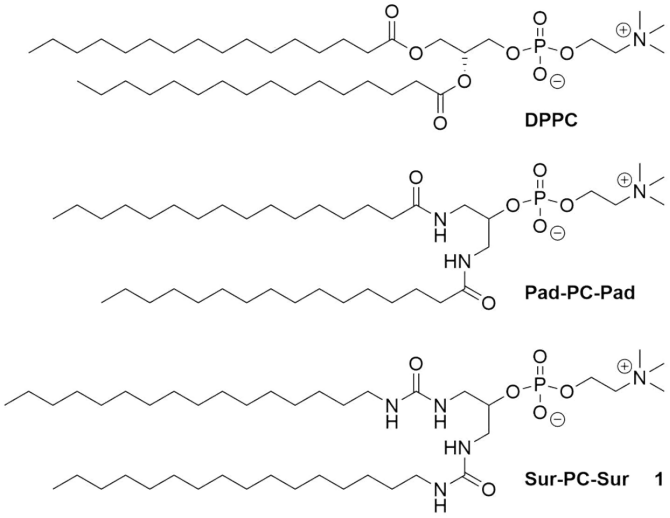

Figure S1. Molecular structure of the natural phospholipid DPPC, the artificial 1,3-diamido phospholipid Pad-PC-Pad and the artificial 1,3-diurea phospholipid Sur-PC-Sur (**1**).

2. Synthesis of *tert*-butyl (2-((amino((1,3-dichloropropan-2-yl)oxy)phosphoryl)oxy) ethyl)carbamate (2)

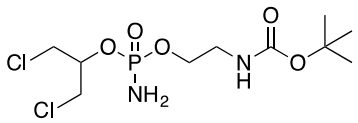

Following our literature procedure[1] NEt_3 (7.0 mL, 494.1 mg, 50.0 mmol) was added to a solution of $POCl_3$ (5.9 mL, 7.7 g, 50.0 mmol) in Et_2O (120 mL). Then the reaction was cooled to 0 °C and 1,3-dichloro-2-propanol (4.8 mL, 6.5 g, 50.0 mmol) was added dropwise. The reaction mixture was stirred for 4.75 h. The mixture was filtered and washed with Et_2O (3 x 40 mL). The solvent was removed under reduced pressure to afford a lightly yellow oil, which was used without further purification.
The oil was dissolved in DCM (80 mL), NEt_3 (7.0 mL, 5.1 mg, 50.0 mmol) was added and afterwards the mixture was cooled to 0 °C. *N*-Boc-ethanolamine (8.1 mg, 7.7 ml, 50 mmol) dissolved in DCM (20 mL) was added dropwise during 2 h. After the addition, the reaction mixture was stirred for further 4.5 h at RT. The reaction mixture was quenched with NH_4OH (90 mL, 25 %) at 0 °C and afterwards it was stirred for further 30 min at RT. The phases were separated and the organic layer was washed with saturated NH_4Cl (40 mL). The aqueous layer was extracted with DCM (3 x 40 mL). The combined organic layers were dried over Na_2SO_4 and concentrated under reduced pressure. The product was purified by silica gel column chromatography (SiO_2, EtOAc). A white powder was obtained (7.35 g, 20.9 mmol, 42 %).

^{1}H-NMR: (300 MHz; $CDCl_3$, δ): 5.06 (s br, 1H), 4.77–4.67 (m, 1H), 4.19–4.04 (m, 2H), 3.88–3.76 (m, 4H), 3.51–3.33 (m, 2H), 3.11 (d, *J* = 4.8 Hz, 2H), 1.43 (s, 9H).
^{31}P-NMR: (121 MHz; $CDCl_3$, δ): 9.1.
***R*$_f$** (EtOAc): 0.27.

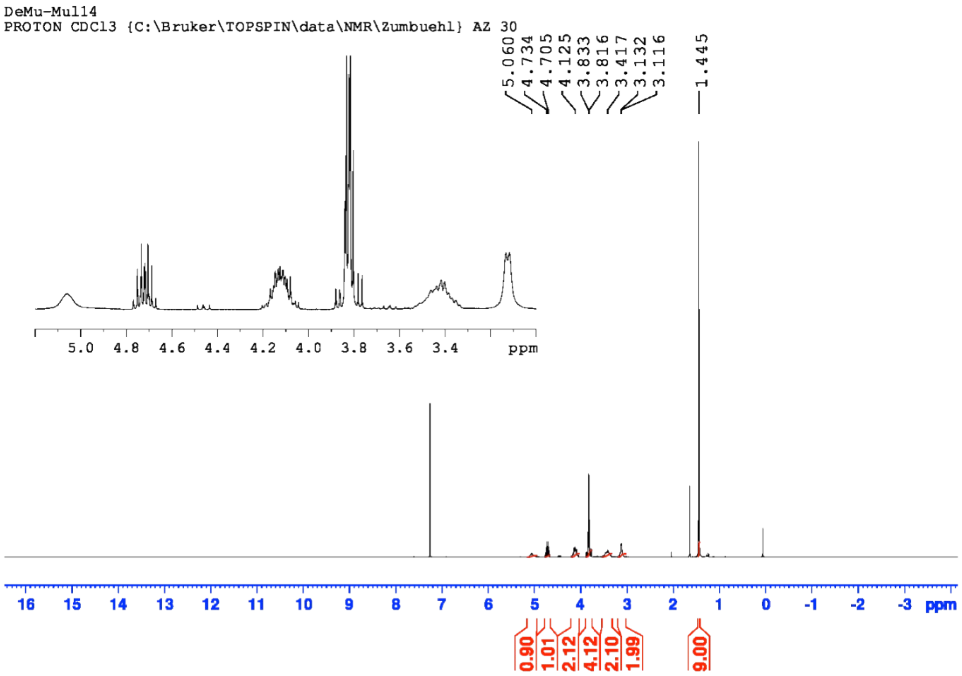

Figure S2. ^{1}H-NMR spectrum of *tert*-butyl (2-((amino((1,3-dichloropropan-2-yl)oxy)phosphoryl) oxy) ethyl)carbamate (**2**).

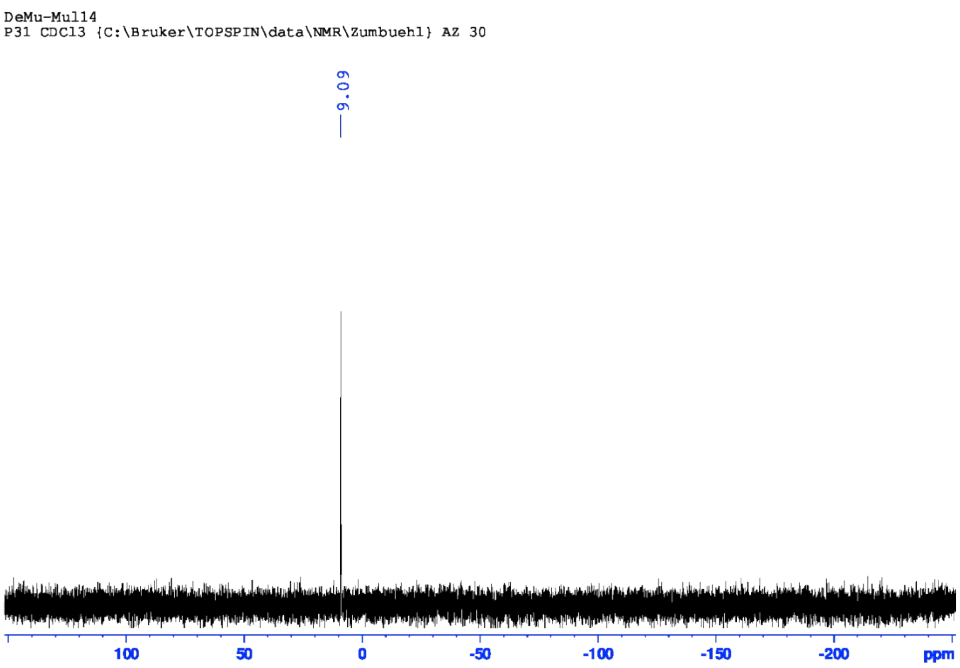

Figure S3. ^{31}P-NMR spectrum of *tert*-butyl (2-((amino((1,3-dichloropropan-2-yl)oxy)phosphoryl) oxy) ethyl)carbamate (**2**).

3. Synthesis of *tert*-butyl (2-((amino((1,3-bis(3-hexadecylurea) propan-2-yl)oxy)phosphoryl)oxy)ethyl)carbamate (3)

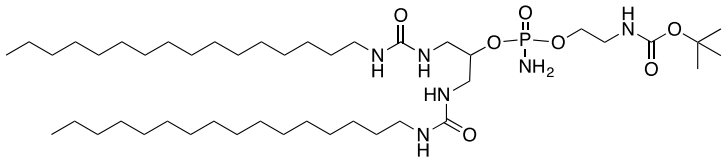

The dichlorophosphoramidite **2** (500.1 mg, 1.43 mmol) was dissolved in DMSO (35 mL) and NaN_3 (250 mg, 3.83 mmol) was added and the resulting solution was heated to 100 °C overnight. Afterwards it was cooled to RT. Brine (30 mL) was added and the solution was extracted with Et_2O (25 mL). The aqueous phase was washed with Et_2O (4 x 25 mL). The combined organic phases were dried over Na_2SO_4. MeOH (50 mL) was added and Et_2O was removed under reduced pressure. The crude diazide, still solved in MeOH, was used without further purification.
Palladium on charcoal (75 mg) was added to the solution of the crude product in MeOH. H_2 was bubbled through the solution (one filled balloon). Afterwards a second balloon filled with H_2 was added and the solution was stirred overnight. To get rid of the Pd-catalyst the solution was filtered over celite and washed with MeOH (3 x 30 mL). The solvent was removed under reduced pressure. The resulting crude diamine was used without further purification.
The crude product was solved in acetonitrile (20 mL) and NEt_3 (5 mL, 3.63 g, 35.8 mmol) was added and the mixture was heated to 40 °C. Afterwards hexadecylisocyanate (765 mg, 0.89 mL, 2.86 mmol) was added slowly and it was stirred for 3 h at 40 °C. After cooling to room temperature, the reaction mixture was filtered and the filtrate was washed with DCM (30 mL). The solvents were removed under reduced pressure and the crude product was purified by column chromatography (silica gel; EtOAc / MeOH, 9:1). The product was isolated as a white wax (825.0 mg, 0.97 mmol, 68 %).

^{1}H-NMR: (300 MHz; $CDCl_3$, δ): 6.11 (s br, 1H), 6.03 (s br, 1H), 5.70 (s br, 1H), 5.38 (s br, 1H), 5.17 (s, 1H), 4.31 (s br, 1H), 4.15–4.00 (m, 4H), 3.90–3.89 (m, 1H), 3.37–3.32 (m, 4H), 3.14–3.07 (m, 4H), 1.43 (s, 13H), 1.24 (s, 52H), 0.89 (t, 6H).
^{31}P-NMR: (121 MHz; $CDCl_3$, δ): 10.2.

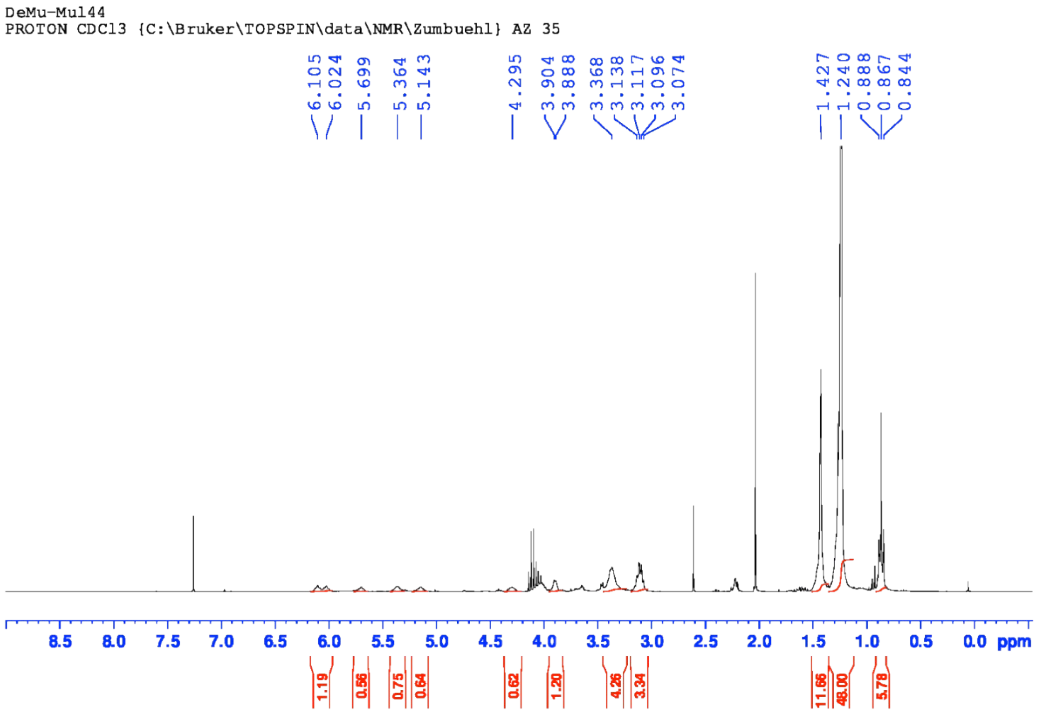

Figure S4. ^{1}H-NMR of tert-butyl (2-((amino((1,3-bis(3-hexadecylurea)propan-2-yl)oxy)phosphoryl)oxy)ethyl)carbamate (**3**).

4. Synthesis of 1,3-bis(3-hexadecylurea)propan-2-yl (2-(trimethylammonio) ethyl)phosphate, Sur-PC-Sur (1)

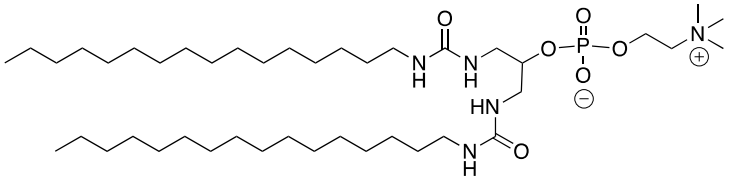

N-Boc-protected Sur-PE-Sur **3** (1.67 g, 2.11 mmol) was dissolved in HCl in Et_2O (1 M, 15 mL) plus a few drops of water. It was stirred for 1.5 h at room temperature. The solvents were removed under reduced pressure.
Sur-PE-Sur was dissolved in MeOH (30 mL). Dimethyl sulfate (1.45 mL, 1.93 g, 15.3 mmol) was added and the mixture was heated up to 40 °C. A K_2CO_3 solution (2.11 g, 15.3 mmol, in 20 mL water) was added and the mixture was stirred at 40 °C for 1 h. After cooling down to room temperature the solvents were removed under reduced pressure, the crude product was purified by column chromatography (silica, DCM / MeOH / H_2O, 65:25:4) and precipitated from $CHCl_3$ / MeOH (1:1) with acetone. A white powder was obtained (500 mg, 0.63 mmol, 30 %).

^{1}H NMR (400 MHz, $CDCl_3$, δ): 6.51 (N*H*, br s, 2H), 5.82 (N*H*, br s, 2H), 4.35 (CH_2, br s, 2H), 4.11 (C*H*, br s, 1H), 3.82 (CH_2, br s, 2H), 3.42–3.35 (CH_2, m, 2H), 3.30 (CH_3, s, 9H), 3.21 (d, *J* = 7.1 Hz, 2H), 3.05 (CH_2, br s, 4H), 1.46–1.36 (CH_2, m, 4H), 1.25 (CH_2, s, 52), 0.87 (CH_3, t, *J* = 6.7 Hz, 6H).
^{13}C NMR (100 MHz, $CDCl_3$, δ): 159.5, 54.4, 50.7, 40.6, 32.1, 30.8, 29.9, 29.9, 29.9, 29.9, 29.8, 29.7, 29.5, 27.3, 22.8, 14.3.
^{31}P NMR (162 MHz, $CDCl_3$, δ): –1.3.
HRMS (m/z): [M+H$^+$] calcd for [M+H], 790.6550; found, 790.6541.
IR: 2916, 2849, 1634, 1564, 1466, 1209, 1056, 1003, 755, 579 cm^{-1}.
R_f (DCM / MeOH / H_2O, 65 : 25 : 4, v:v:v): 0.67.

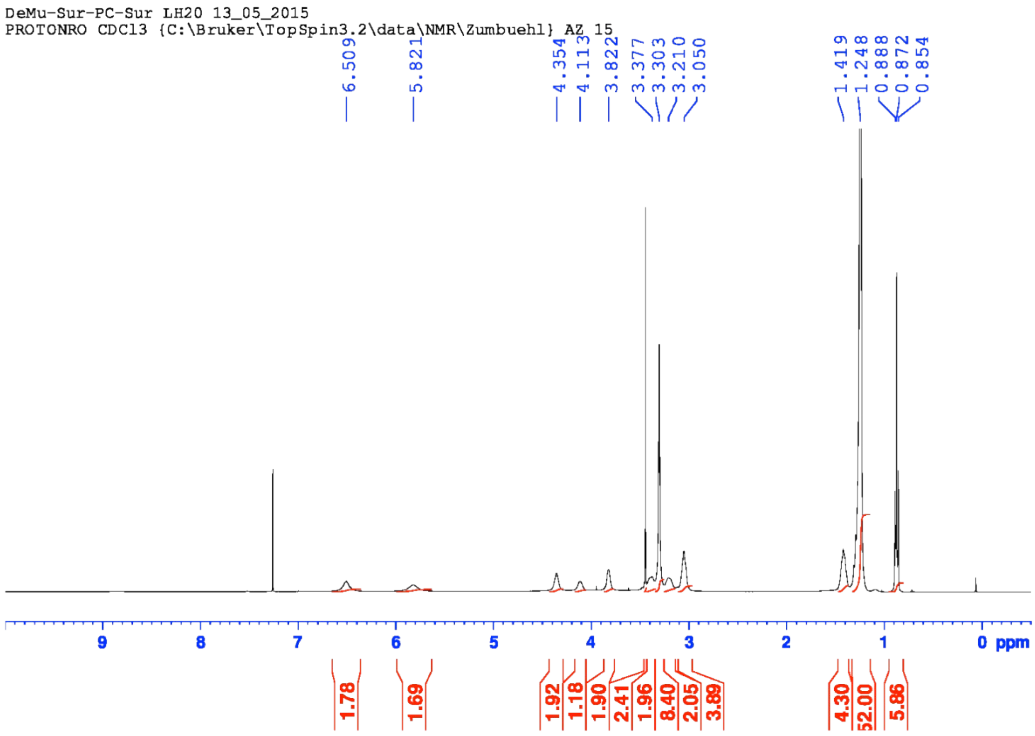

Figure S5. ^{1}H-NMR of Sur-PC-Sur (**1**).

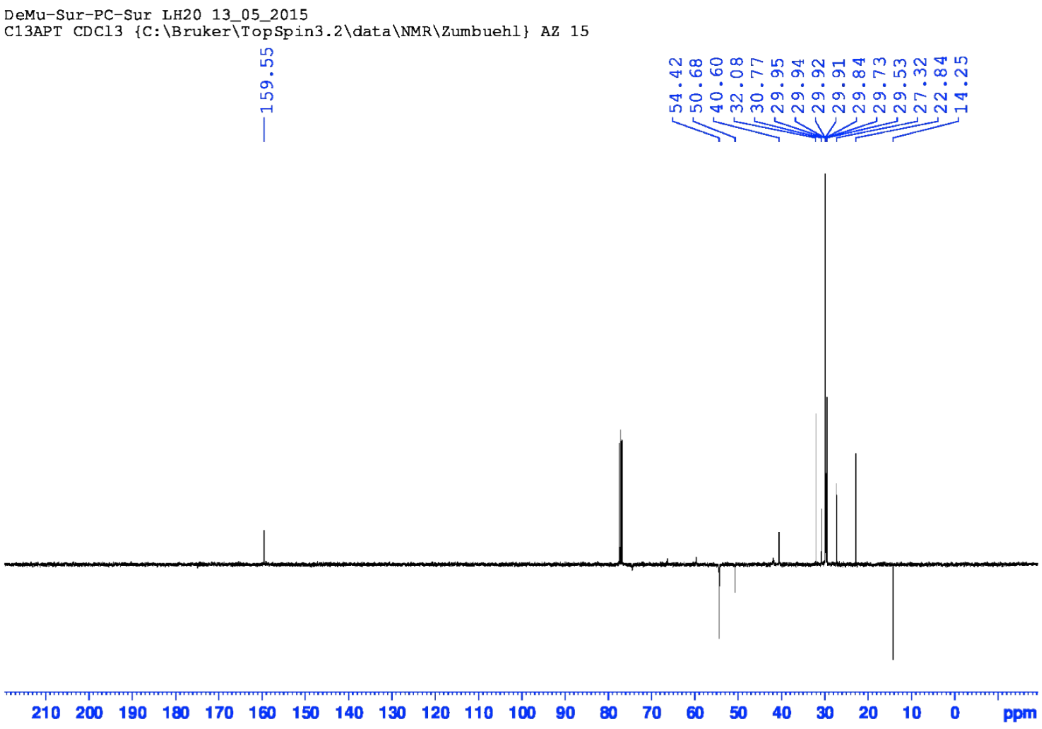

Figure S6. ^{13}C-NMR of Sur-PC-Sur (**1**).

5. Differential Scanning Calorimetry

Adapted from.[2] Multilamellar vesicle suspensions were prepared by hydration of 1 mg of phospholipid powder with 1 mL of ultra-pure water (18.2 MΩ·m). The unextruded vesicle suspensions were degassed for 30 minutes using a TA degassing station. The alternative heating-cooling scans were recorded from 5 °C to 90 °C with a scanning speed of 0.5 °C/min. The experiment was performed twice, starting with new suspensions, in order to ensure reproducibility. The scans of the second heating-cooling scans are reported. Raw data was baseline corrected and converted to molar heat capacity (MHC) using the NanoAnalyze software (TA Instruments, USA). The main phase transition and enthalpy were determined with the same software and verified using the OriginLab software (OriginLabs, USA).

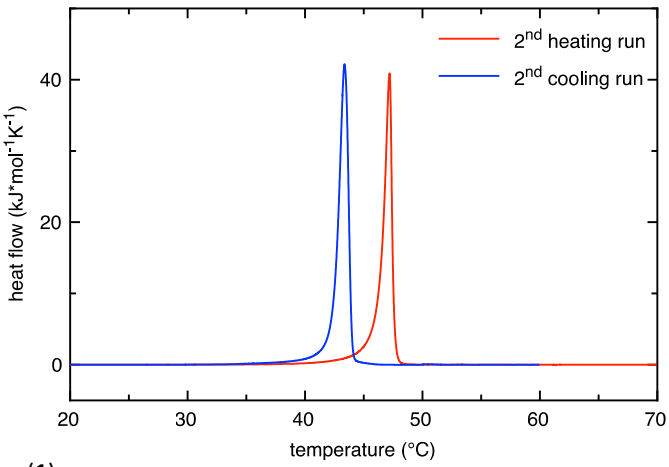

Figure S7. DSC traces of Sur-PC-Sur (**1**).

6. Small-Angle and Wide-Angle X-ray Scattering

Adapted from.[3] A lipid dispersion (MLV, 20 wt% in ultra-pure water) was transferred into glass capillaries (inner diameter 2 mm, GLAS, Germany). The small angle X-ray scattering (SAXS) was carried out at the in-house pinhole Instrument with rotating anode. The diffracted signal has been measured with a Mar CCD plate detector (Evanston, Illinois, USA). The incoming beam had a wavelength of 154 pm, and the exposure time was 2 h. The temperature was fixed at 21 °C during measurements. Positions of the Bragg peaks were converted into real space repeat distances of the lattice planes. In order to determine peak maxima and the full-width at half-maximum (FWHM) Lorentzian curves have been fitted to the experimental points.

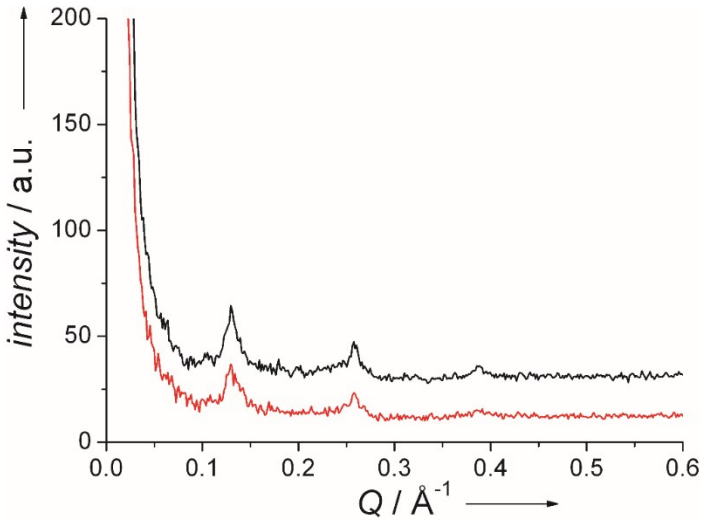

Figure S8. Small-angle X-ray scattering at lower Q values with a vertical (red) or horizontal (black) orientation of the capillary. The scattering vector's maximum Q is 0.1292 $Å^{-1}$ (black) and 0.1293 $Å^{-1}$. The resulting mean d value is 48.6 Å for an interdigitated lamellar phase.

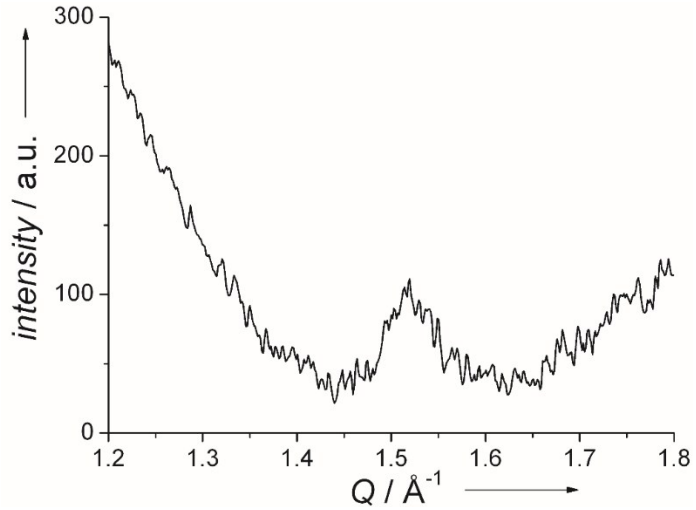

Figure S9. Wide X-ray scattering measurement with the scattering vector's maximum Q at 1.518 $Å^{-1}$ corresponding to a hexagonal chain packing with an area per acyl chain of 19.8 $Å^2$.

7. Vesicle Preparation

Adapted from.[2] $LUVET_{100}$ of Sur-PC-Sur (**1**) were prepared following the standard extrusion protocol: In a 25 ml round bottom flask, 10 mg of the lipid were dissolved in CH_2Cl_2. After evaporation of the organic solvent, the film was further dried under high vacuum (40 mbar) overnight. Then the film was hydrated with the internal buffer for 30 min. (1 ml, 50 mM 5(6)-carboxyfluorescein, 10 mM HEPES buffer (AppliChem), 10 mM NaCl dissolved in pure water, pH 7.4 (NaOH)). Now at least 5 freeze-thaw cycles (liquid N_2 to 65 °C) were carried out before the suspension was extruded 11 times using a Mini Extruder (Avanti Polar Lipids, USA) using track-edged filters with a mesh size of 100 nm (Whatman, USA). The external buffer was then exchanged on a size exclusion column (1.5 × 20 cm Sephadex G-50 column) in external buffer (107 mM NaCl, 10 mM HEPES dissolved in ultrapure water, pH 7.4 (NaOH)).

8. Cryogenic Transmission Electron Microscopy

Adapted from.[4] $LUVET_{100}$ of Sur-PC-Sur (**1**) were prepared by the extrusion protocol described above at a concentration of 10 mg/ml. The liposome suspensions were let to reach room temperature and were diluted 1:1 with isotonic saline and were mounted on glow-discharged holey carbon grids, quickly frozen by a Cryoplunge 3 system (Gatan, USA) and transferred to a JEM2200FS transmission electron microscope (JEOL, Japan) using a Gatan626 cryo-holder. Cryo-electron micrographs were recorded at the acceleration voltage of 200 kV, x 20,000 magnification, 4–8 µm underfocus and a dose of 10 electrons/Å^2, using a F416 CMOS detector (TVIPS, Germany). The final concentration of the liposomal suspension used was 5 mg/ml or 6.3 mM.
The thickness of the bilayer was measured using the open source software Fiji.[5-7]

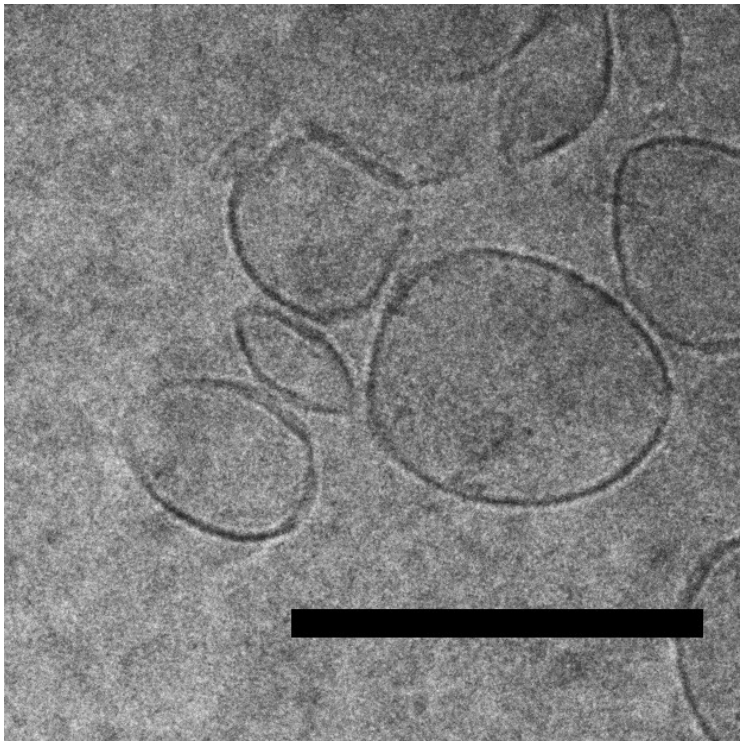

Figure S10. Magnification of a cryo transmission electron micrograph of Sur-PC-Sur (**1**) showing the bimodal distribution of faceted and non-faceted vesicles and the presence of non-vesicle material. The scale bar has a length of 200 nm. Full overview micrographs are shown in the supporting information.

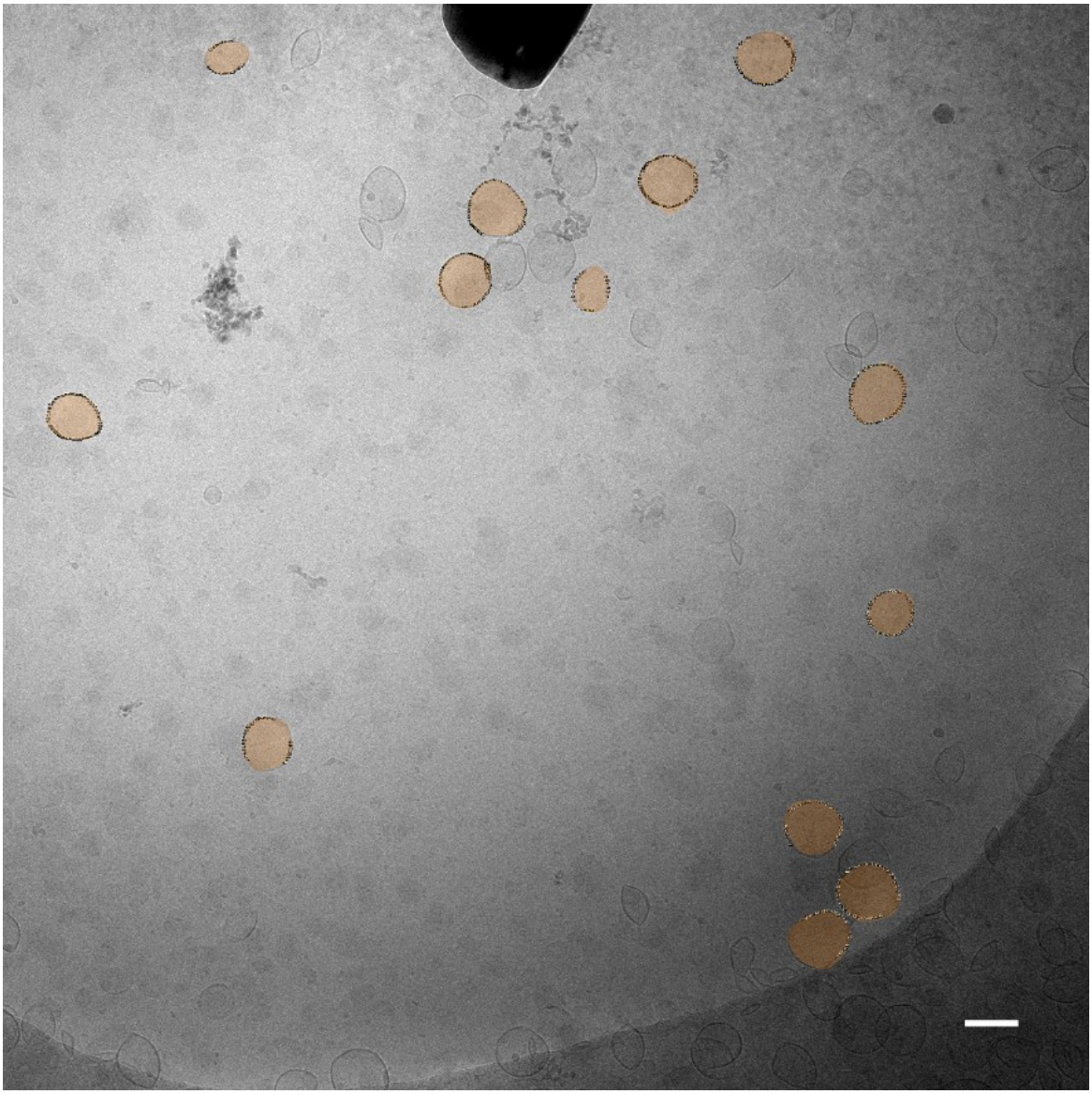

Figure S11. Cryo TEM image of Sur-PC-Sur (**1**) containing vesicles. Highlighted are the vesicles that were used to measure the membranes' thickness for spherical structures. The total number of measured cross-sections was 505. The scale bar is 200 nm long.

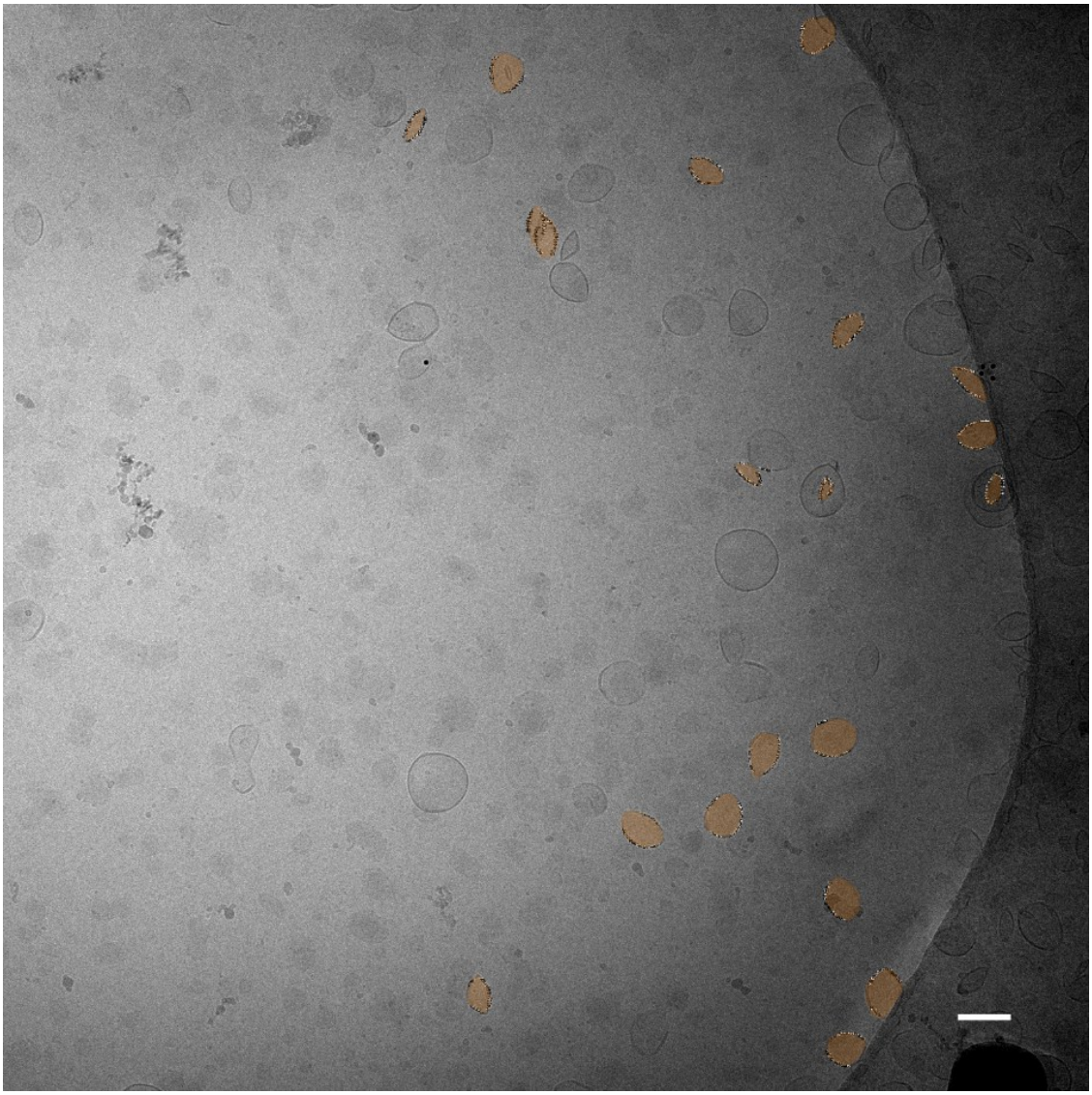

Figure S12. Cryo TEM image of Sur-PC-Sur (**1**) containing vesicles. Highlighted are the vesicles that were used to measure the membranes' thickness for facetted structures. The total number of measured cross-sections was 468. The scale bar is 200 nm long.

9. Release Experiments

Adapted from.[2] The inner buffer (CF buffer) was prepared from 50 mM 5(6)-carboxyfluorescein (powder, Sigma-Aldrich) and 10 mM HEPES buffer (powder, Sigma-Aldrich) dissolved in ultra-pure water (18.2 MΩ·cm). The pH was adjusted to 7.4 (NaOH) and the osmotic concentration to 200 mOs/mL (NaCl). The outer buffer was prepared from 10 mM HEPES buffer (powder, Sigma-Aldrich) dissolved in ultra-pure water (18.2 MΩ·cm). The pH was adjusted to 7.4 (NaOH) and the osmotic concentration to 200 mOs/mL (NaCl). Sur-PC-Sur (**1**) (2 mg) was weighed into a round-bottomed flask (25 mL) and dissolved in $CHCl_3$ (1 ml, amylene stabilized, Sigma-Aldrich, USA). The solvent was removed by low-pressure rotatory evaporation. The thin film was dried under high vacuum overnight, to ensure the removal of residual water and prevent cholesterol oxidation. Inner buffer (1 mL) was added to the round- bottomed flask and the film was hydrated for 30 minutes at 65 °C. The film was subjected to five cycles of freeze/thaw using liquid nitrogen and a 65 °C water bath. The resulting MLV suspension was extruded 11 times through a track-etched filter membrane at 65 °C (100 nm, Whatman, USA) placed in a Mini Extruder (Avanti Polar Lipids, USA). The vesicles were left standing at room temperature overnight. The residual non-encapsulated CF buffer, in the $LUVET_{100}$ suspension, was exchanged with the outer buffer using size exclusion chromatography (PD-10 desalting columns, GE Healthcare, UK). The size exclusion chromatography was carried out after 24 hours storage, in the dark at room temperature, of the $LUVET_{100}$ suspension.

The purified $LUVET_{100}$ suspension was diluted, in a volumetric flask, to 100 mL using additional outer buffer. Six aliquots (2 mL) were separated into vials (5 ml, PE caps) and vortex mixed for different amounts of time (0, 5, 10, 20, 30, 60 s) at 2500 rpm. The 5(6)-carboxyfluorescein release was quantified using a fluorospectrometer (Sense 425–301, Hidex, Finland). For each sample, five microplate wells were filled with 200 µl of the vortex 20 mixed vesicular suspension. The wavelengths used for measurements were 485 nm (excitation) and 535 nm (emission). As a control for the maximum dye release (F100), a Triton X-100 solution (2 µl of a 10 vol% solution) was added to additional five microplate wells, filled with 200 µl of vesicular suspension, for each sample. The release fraction at time X was calculated with the formula:

$$Release\ (\%) = \frac{F_X - F_0}{F_{100} - F_0}$$

where F_X is the fluorescence at time X, F_0 the fluorescence at time zero and F_{100} the maximum fluorescence recorded after treatment with Triton X-100.

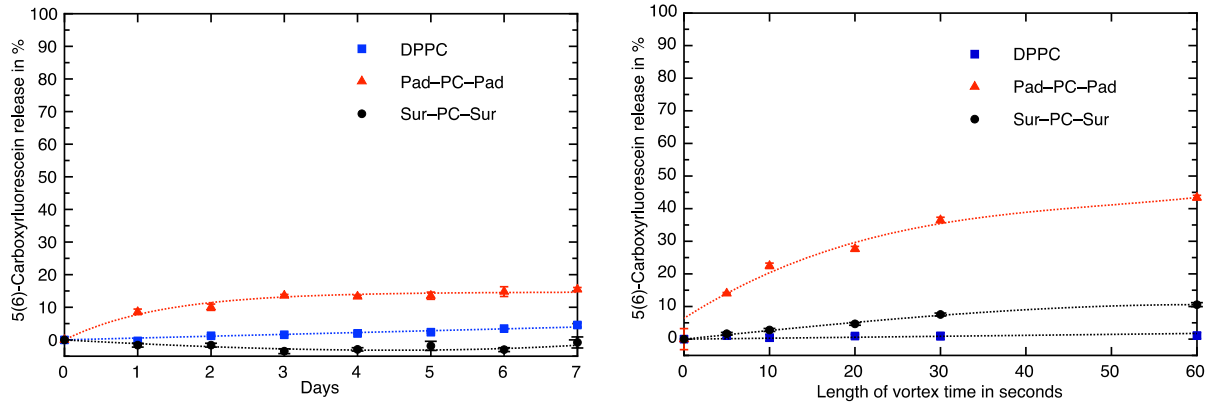

Figure S13. Left: spontaneous release of vesicle-entrapped 5(6)-carboxyfluorescein upon prolonged storage of the vesicles at room temperature. Right: Release of the vesicle-entrapped dye upon vortex shaking. Data for DPPC and Pad-PC-Pad were already published in.[8] Fitted lines are for guiding the eyes only.

10. Film Balance Measurements

Adapted from.[2] Pressure-area isotherms were recorded on a computer interfaced Langmuir trough with a surface area of 194 cm^2 (Riegler & Kierstein, Potsdam, Germany). The paper plate Wilhelmy method was used to measure the surface tension with an accuracy of ±0.1 mN/m. Each measurement was repeated at least three times. The Langmuir trough was filled with ultrapure water (specific resistance of 18.2 MΩ·cm). The lipid solution (1 mg/ml) in chloroform was spread and the measurement was started 5–15 min after spreading.
The isothermal surface compressional modulus K is defined as:

$$K = -A\left(\frac{\partial \pi}{\partial A}\right)_T$$

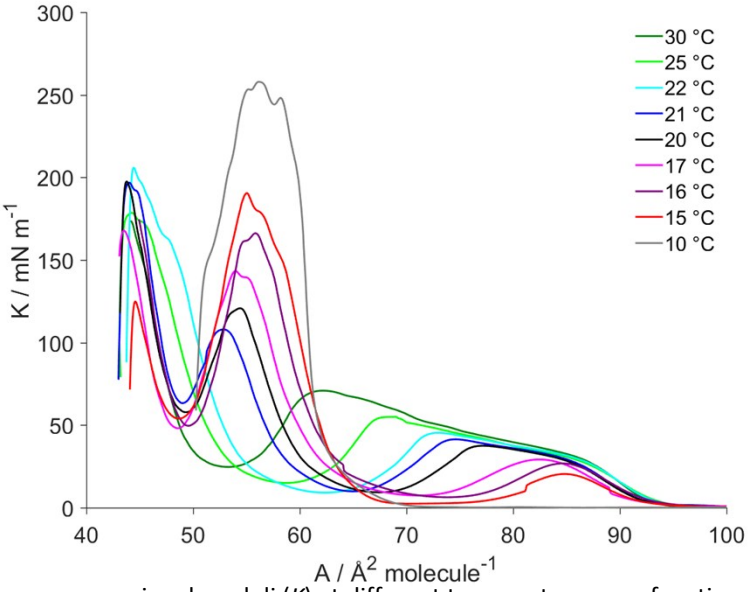

Figure S14. Isothermal surface compressional moduli (*K*) at different temperatures as a function of area per molecule.

11. Grazing Incidence X-ray Diffraction Measurements

Adapted from.[4] The lattice structure of the monolayers was investigated using the liquid surface diffractometer at the undulator beamline BW1 (HASYLAB, DESY, Hamburg, Germany) by grazing incidence X-ray diffraction (GIXD) measurements. At BW1, a Langmuir film balance equipped with a Wilhelmy plate was positioned in a hermetically closed container flushed with helium. A monochromatic synchrotron X-ray beam (λ = 1.304 Å) was adjusted to strike the helium/water interface at a grazing incidence angle $\alpha_i = 0.85\alpha_c$ ($\alpha_c = 0.13°$) lighting up roughly 2×50 mm² of the surface. The trough was laterally moved during the measurements to prevent any sample damage by the strong X-ray beam. For the measurement of the diffracted signal a MYTHEN detector system (PSI, Villigen, Switzerland) was rotated to scan the in-plane Q_{xy} component values of the scattering vector. The vertical strips of the MYTHEN measured the out-of-plane Q_z component of the scattering vector between 0.0 and 0.75 $Å^{-1}$. The diffraction data consisted of Bragg peaks at diagnostic Q_{xy} values. The diffracted intensity normal to the interface was integrated over the Q_{xy} window of the diffraction peak to calculate the corresponding Bragg rod.

Table S1. Top: Bragg peak (Q_{xy}) and Bragg rod (Q_z) positions and the corresponding full-widths at half-maximum of Sur-PC-Sur (**1**) monolayers at different surface pressures π and 10 °C. Bottom: Lattice parameters of Sur-PC-Sur (**1**) monolayers at 10 °C.

π [mN/m]	Q_{xy} [$Å^{-1}$]	Q_z [$Å^{-1}$]	Q_{xy} [$Å^{-1}$]	Q_z [$Å^{-1}$]	Q_{xy} [$Å^{-1}$]	Q_z [$Å^{-1}$]
2	1.541 0.013	0.373 0.30	1.214 0.020	0.791 0.30	1.038 0.034	1.164 0.30
12	1.546 0.010	0.388 0.29	1.224 0.027	0.767 0.3	1.057 0.062	1.155 0.3
22	1.550 0.054	0.387 0.29	1.230 0.036	0.768 0.3	1.069 0.064	1.155 0.3
22	1.510 0.052	0 0.29	1.346 0.107	0.70 0.28		
32	1.515 0.051	0 0.29	1.374 0.102	0.625 0.28		
32	1.515 0.051	0 0.29	1.346 0.088	0.662 0.28		
42	1.534 0.093	0 0.29	1.359 0.096	0.663 0.28		
42	1.534 0.093	0 0.29	1.382 0.091	0.614 0.28		

π [mN/m]	a/b/c [Å]	α/β/γ [°]	distortion	tilt [°]	A_{xy} [$Å^2$]	A_0 [$Å^2$]
2	5.188 6.068 7.703	137.8 128.2 94.0	0.4674923	51.6	31.4	19.5
12	5.153 5.967 7.537	137.1 127.9 95.0	0.4521226	50.6	30.6	19.4
22	5.132 5.905 7.441	136.6 127.8 95.5	0.4434249	50.2	30.2	19.3
22	5.639 5.026 5.026	111.8 124.1 124,1	0.1586793	32.1	23.5	19.9
32	5.481 4.971 4.971	113.1 123.5 123.5	0.1341955	28.6	22.7	20.0
32	5.647 5.017 5.017	111.5 124.2 124.2	0.1633847	30.7	23.4	20.1
42	5.601 4.962 4.962	111.3 124.4 124.4	0.1674490	30.6	22.9	19.7

42	5.465 4.923 4.924	112.6 123.7 123.7	0.1436034	28.1	22.4	19.7

Table S2. Top: Bragg peak (Q_{xy}) and Bragg rod (Q_z) positions and the corresponding full-widths at half-maximum of Sur-PC-Sur (**1**) monolayers at different surface pressures π and 10 °C. Bottom: Lattice parameters of Sur-PC-Sur (**1**) monolayers at 20 °C.

π [mN/m]	Q_{xy} [Å^{-1}]	Q_z [Å^{-1}]	Q_{xy} [Å^{-1}]	Q_z [Å^{-1}]	Q_{xy} [Å^{-1}]	Q_z [Å^{-1}]
12	1.489 0.029	0 0.30	1.336 0.103	0.697 0.29		
16	1.492 0.013	0 0.29	1.392 0.047	0.590 0.29		
30	1.492 0.055	0 0.29	1.363 0.135	0.616 0.29		
40	1.498 0.042	0 0.30	1.428 0.108	0.449 0.30		

π [mN/m]	a/b/c [Å]	α/β/γ [°]	dist. (NN)	tilt [°]	A_{xy} [Å^2]	A_0 [Å^2]
12	5.664 5.082 5.082	112.3 123.9 123.9	0.1493801	32.1	23.9	20.2
16	5.346 4.988 4.988	115.2 122.4 122.4	0.09453582	26.7	22.5	20.1
30	5.508 5.032 5.032	113.6 123.2 123.2	0.1239716	28.4	23.2	20.4
40	5.168 4.926 4.926	116.7 121.6 121.6	0.06479216	20.3	21.7	20.3

Table S3. Top: Bragg peak (Q_{xy}) and Bragg rod (Q_z) positions and the corresponding full-widths at half-maximum of Sur-PC-Sur (**1**) monolayers at different surface pressures π and 10 °C. Bottom: Lattice parameters of Sur-PC-Sur (**1**) monolayers at 24 °C.

π [mN/m]	Q_{xy} [Å^{-1}]	Q_z [Å^{-1}]	Q_{xy} [Å^{-1}]	Q_z [Å^{-1}]	Q_{xy} [Å^{-1}]	Q_z [Å^{-1}]
22	1.487 0.023	0 0.30	1.366 0.122	0.638 0.29		
30	1.489 0.035	0 0.30	1.400 0.124	0.535 0.30		
40	1.504 0.015	0 0.29	1.469 0.067	0.324 0.29		

π [mN/m]	a/b/c [Å]	α/β/γ [°]	dist. (NN)	tilt [°]	A_{xy} [Å^2]	A_0 [Å^2]
22	5.483 5.037 5.037	114.0 123.0 123.0	0.1161730	29.1	23.2	20.2
30	5.299 4.983 4.983	115.7 122.1 122.1	0.08379202	24.3	22.4	20.4
40	4.979 4.863 4.863	118.4 120.8 120.8	0.03163751	14.4	20.8	20.1

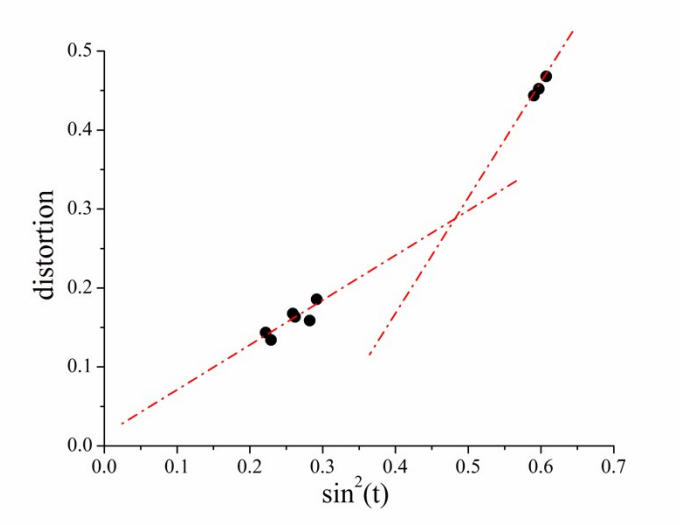

Figure S15. Lattice distortion *d* as function of $\sin^2(t)$ of Sur-PC-Sur (**1**) monolayers at 10 °C.

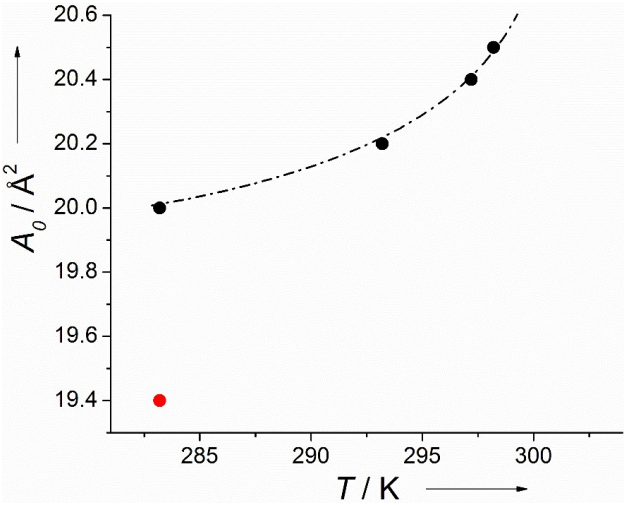

Figure S16. Cross-sectional area A_0 as a function of temperature. ● – LC1 phase, ● – LC2 phase.

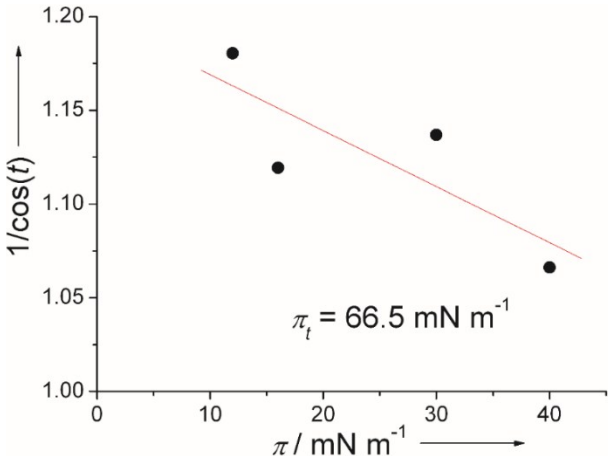

Figure S17. Dependence of the tilt angle of the alkyl chains (*t*) represented as 1/cos(*t*) on the lateral surface pressure (π) at a subphase temperature of 20 °C.

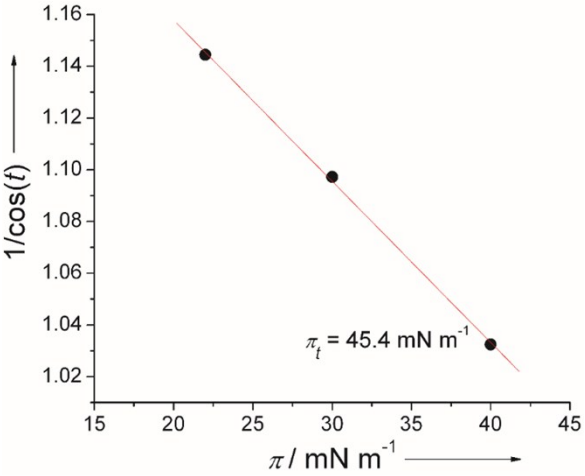

Figure S18. Dependence of the tilt angle of the alkyl chains (*t*) represented as 1/cos(*t*) on the lateral surface pressure (π) at a subphase temperature of 24 °C.

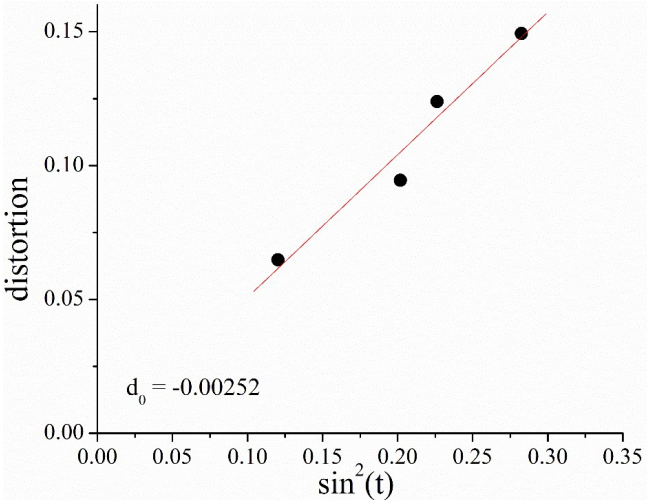

Figure S19. Lattice distortion *d* as function of $\sin^2(t)$ of Sur-PC-Sur (**1**) monolayers at 20 °C.

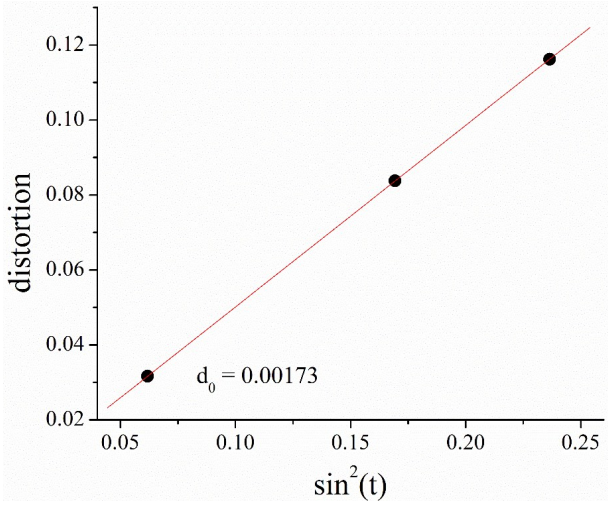

Figure S20. Lattice distortion *d* as function of $\sin^2(t)$ of Sur-PC-Sur (**1**) monolayers at 24 °C.

12. Specular X-ray Reflectivity

Specular X-ray reflectivity (XR) experiments were performed using the same liquid-surface diffractometer on the undulator beamline BW1. The experimental setup and evaluation procedure have been described in detail elsewhere.[9-11] XR experiments reveal information on the electron-density distribution along the surface normal and may be used to determine the thickness of thin layers. The reflected intensity was measured by a NaI scintillation detector as a function of the vertical incidence angle, αi, with the geometry $\alpha_i = \alpha_f = \alpha$, where α_f is the vertical exit angle of the reflected X-rays. The vertical scattering vector component $Q_z = (4\pi/\lambda)\sin(\alpha_f)$ was measured in a range between 0.01 - 0.6 $Å^{-1}$. The background scattering from, e.g., the subphase was measured at $2\theta_{hor} = 0.7°$ and subtracted from the signal measured at $2\theta_{hor} = 0°$. The reflectivity data were inverted by applying a model-independent approach.[12] The obtained electron density profile was interpreted by applying a box model.

13. Infrared Reflection-Absorption Spectroscopy

Adapted from.[4] Infrared reflection-absorption spectra were recorded using the Vertex 70 FT-IR spectrometer (Bruker, Germany), equipped with a liquid-nitrogen cooled MCT detector and coupled to a Langmuir film balance, which was placed in a sealed container (an external air/water reflection unit (XA-511, Bruker)) to guarantee a constant vapor atmosphere. Using a KRS-5 (thallium bromide and iodide mixed crystal) wire grid polarizer, the IR-beam was polarized parallel (p) or vertical (s) and focused on the fluid subphase at an angle of incidence of 40°.

A computer controlled "trough shuttle system" enables us to choose between the compartment with the sample (subphase with spread layer) and a reference compartment (pure subphase). The single-beam reflectance spectrum from the reference trough was taken as background for the single-beam reflectance spectrum of the monolayer in the sample trough to calculate the reflection absorption spectrum as $-\log(R/R_0)$ in order to eliminate the water vapor signal. FTIR spectra were collected at a resolution of 8 cm^{-1} using 200 scans for s-polarized light and 400 scans for p-polarized light.

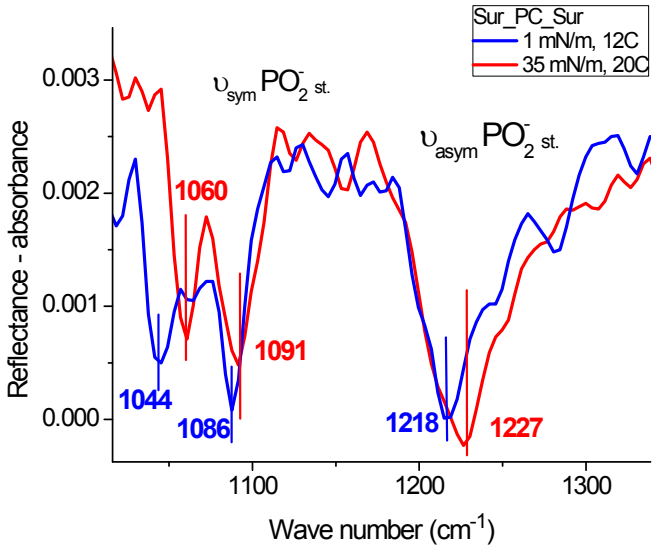

Figure S21. IRRA spectra of Sur-PC-Sur monolayers measured at 12 °C and 1 mN/m (blue line) and at 20 °C and 35 mN/m (red line).

14. Brewster-Angle Microscopy

Adapted from.[13] Brewster angle micrographs were recorded with a commercially available Multiskop (Optrel, Germany) equipped with a Langmuir trough from Riegler & Kierstein constructed identically to the one described above. Great care was taken that the investigated films were prepared under the same experimental conditions as for the monolayers that have already been discussed in this article.

Parallel polarized laser light with respect to the plane of incidence of a wavelength of λ = 632.8 nm is reflected on the water surface under the Brewster angle of water (53.1°). The polarizer and analyzer were set to 0° to suppress reflected light from a pure water surface. The reflected beam, which maps the inhomogeneities of the Langmuir film, is focused on a CCD camera for visualization. An objective of 10-fold magnification (Mitutoyo) is mounted on a piezo translation stage that moves continuously to bring consecutive stripes of the image into focus. A streaming video sequence is recorded to construct an overall sharp image. The lipid films were imaged at different stages of monolayer compression.

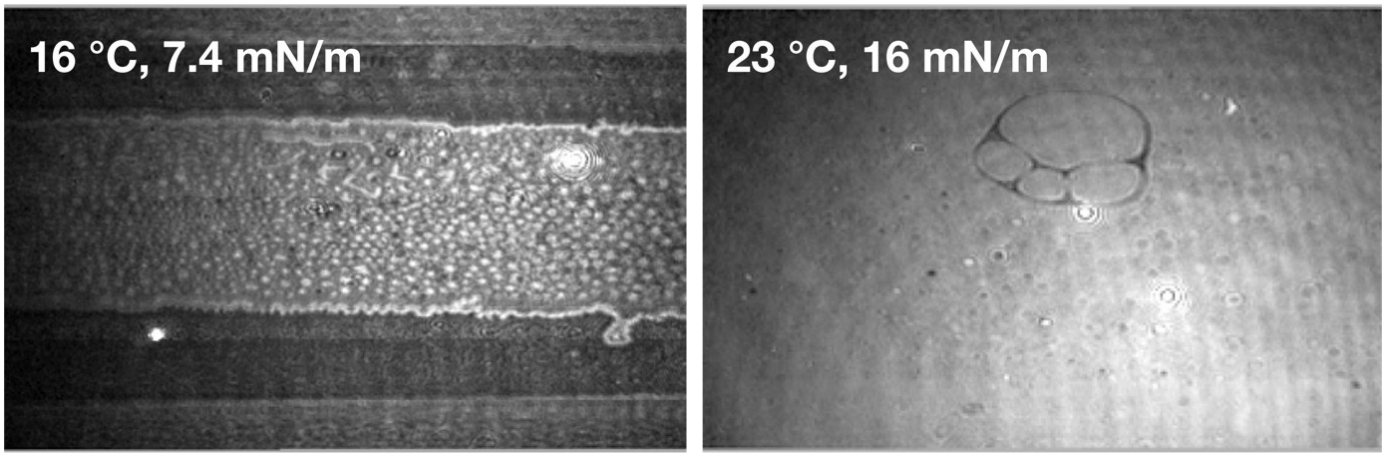

Figure S22. Brewster-angle microscopy of LC1 (left) and LC2 (right). Both images have a resolution of 5.35 µm x 5.10 µm.

15. References

1. Fedotenko, I. A.; Zaffalon, P. L.; Favarger, F.; Zumbuehl, A., The synthesis of 1,3-diamidophospholipids. *Tetrahedron Lett.* **2010,** *51* (41), 5382–5384.
2. Neuhaus, F.; Mueller, D.; Tanasescu, R.; Balog, S.; Ishikawa, T.; Brezesinski, G.; Zumbuehl, A., Vesicle Origami: Cuboid Phospholipid Vesicles Formed by Template-Free Self-Assembly. *Angew. Chem. Int. Ed.* **2017,** *56* (23), 6515–6518.
3. Weinberger, A.; Tanasescu, R.; Stefaniu, C.; Fedotenko, I. A.; Favarger, F.; Ishikawa, T.; Brezesinski, G.; Marques, C. M.; Zumbuehl, A., Bilayer Properties of 1,3-Diamidophospholipids. *Langmuir* **2015,** *31* (6), 1879–1884.
4. Fedotenko, I. A.; Stefaniu, C.; Brezesinski, G.; Zumbuehl, A., Monolayer Properties of 1,3-Diamidophospholipids. *Langmuir* **2013,** *29* (30), 9428–9435.
5. Schneider, C. A.; Rasband, W. S.; Eliceiri, K. W., NIH Image to ImageJ: 25 years of image analysis. *Nat. Methods* **2012,** *9* (7), 671–675.
6. Schindelin, J.; Arganda-Carreras, I.; Frise, E.; Kaynig, V.; Longair, M.; Pietzsch, T.; Preibisch, S.; Rueden, C.; Saalfeld, S.; Schmid, B.; Tinevez, J. Y.; White, D. J.; Hartenstein, V.; Eliceiri, K.; Tomancak, P.; Cardona, A., Fiji: an open-source platform for biological-image analysis. *Nat. Methods* **2012,** *9* (7), 676–682.
7. Schindelin, J.; Rueden, C. T.; Hiner, M. C.; Eliceiri, K. W., The ImageJ ecosystem: An open platform for biomedical image analysis. *Mol. Reprod. Dev.* **2015,** *82* (7-8), 518–529.
8. Holme, M. N.; Fedotenko, I. A.; Abegg, D.; Althaus, J.; Babel, L.; Favarger, F.; Reiter, R.; Tanasescu, R.; Zaffalon, P.-L.; Ziegler, A.; Müller, B.; Saxer, T.; Zumbuehl, A., Shear-stress sensitive lenticular vesicles for targeted drug delivery. *Nat. Nanotechnol.* **2012,** *7*, 536–543.
9. Helm, C. A.; Mohwald, H.; Kjaer, K.; Alsnielsen, J., Phospholipid Monolayer Density Distribution Perpendicular to the Water-Surface - a Synchrotron X-Ray Reflectivity Study. *Europhysics Letters* **1987,** *4* (6), 697–703.
10. Schalke, M.; Kruger, P.; Weygand, M.; Losche, M., Submolecular organization of DMPA in surface monolayers: beyond the two-layer model. *Biochimica Et Biophysica Acta-Biomembranes* **2000,** *1464* (1), 113–126.
11. Jensen, T. R. M.; Kjaer, K., Studies in Interface Science. In *Novel Methods to Study Interfacial Layers*, Moebius, D.; Miller, R., Eds. Elsevier Science: New York, 2001; Vol. 11, pp 205–254.
12. Pedersen, J. S.; Hamley, I. W., Analysis of Neutron and X-Ray Reflectivity Data. II. Constrained Least-Squares Methods. *J. Appl. Cryst.* **1994,** *27*, 36–49.
13. Tanasescu, R.; Lanz, M. A.; Mueller, D.; Tassler, S.; Ishikawa, T.; Reiter, R.; Brezesinski, G.; Zumbuehl, A., Vesicle Origami and the Influence of Cholesterol on Lipid Packing. *Langmuir* **2016,** *32* (19), 4896–4903.

16. Author Contributions

Frederik Neuhaus did the purification and characterization of the phospholipid Sur-PC-Sur (**1**), data analysis and interpretation as well as writing the manuscript. Dr. Dennis Mueller performed the phospholipid synthesis, vesicle preparation for cryo-TEM and SAXS/WAXS experiments and performed the release experiments together with Dr. Radu Tanasescu who also measured the DSC and GIXD together with Dr. Cristina Stefaniu who additionally did the data analysis for the IRRAS experiments. Dr. Sandor Balog measured first SAXS/WAXS data. Prof. Dr. Takashi Ishikawa executed the cryo-TEM experiments at PSI Villigen. Dr. Renate Reiter conducted the BAM measurements. Prof. Dr. Gerald Brezesinski measured SAXS/WAXS/GIXD/XRR and together with Prof. Dr. Andreas Zumbuehl gave scientific guidance for the interpretation process and helped writing the manuscript. Prof. Dr. Andreas Zumbuehl was responsible for the original idea, did the funding acquisition and project administration.